

# Throughput Analysis of UAV-assisted IAB Cellular Networks with Heterogeneous Traffic

Yue Zhang\*, Hangguan Shan\*, Meiyan Song\*, Howard H. Yang<sup>‡</sup>, Qi Zhang<sup>†</sup>, and Xianhua He<sup>†</sup>

\*College of Information Science and Electronic Engineering, Zhejiang University, Hangzhou 310027, China

<sup>‡</sup>ZJU-UIUC Institute, Zhejiang University, Haining 314400, China

<sup>†</sup>Department of ECE, University of Illinois at Urbana-Champaign, Champaign, IL 61820, USA

<sup>†</sup>Nokia Solutions and Networks System Technology (Beijing) Co., Ltd, Hangzhou 310053, China

**Abstract**—With the deluge of wireless data, unmanned aerial vehicles (UAVs) are expected to be deployed as aerial small base stations (SBSs) to relieve the load of ground macro base stations by establishing wireless backhaul connections with them and providing high-quality service to users. Thanks to the emergence of integrated access and backhaul (IAB), the access and backhaul communication links can work on the same millimeter wave (mmWave) band with huge available bandwidth. This paper studies the quality-of-service (QoS) performance of heterogeneous traffic under equal partition and average load partition spectrum allocation strategies for mmWave UAV-assisted IAB cellular networks. Specifically, we develop a theoretical framework to analyze the mean packet throughput (MPT) of users based on stochastic geometry and queueing theory. Simulation results demonstrate that the deployment of UAVs can promote MPT performance compared to ground SBSs and appropriate UAV height, UAV density, and spectrum allocation play significant roles in improving QoS performance of heterogeneous traffic in the network.

## I. INTRODUCTION

With the advantages of mobility, low laying cost, and adaptive altitude, unmanned aerial vehicles (UAVs) are expected to play a vital role as aerial access points (APs) in millimeter wave (mmWave) wireless communication systems [1]. UAVs can avoid obstacles and establish line-of-sight (LoS) communication links with ground user equipments (GUEs) by adjusting their heights, which averts the attenuation of mmWave penetrating obstacles and improves signal quality and communication capability [2]. In UAV-assisted cellular networks, UAVs work as aerial APs to assist ground base stations (BSs) by relieving their loads, while the backhaul links between UAVs and ground BSs become the bottleneck to the service capability of UAVs.

With huge available bandwidth and directional antenna array, mmWave band can achieve fiber-like transmission performance for UAV backhaul links [3]. In [4], UAVs connect to ground BSs through mmWave wireless backhaul while the access links between GUEs and UAVs or BSs work on sub-6G band. Accordingly, UAVs and BSs are needed to equip with two sets of transceivers. The emergence of integrated access and backhaul (IAB) solves the problem, where access and backhaul communication links share the same mmWave band [5]. Thus, an appropriate communication resource allocation strategy is needed to reduce the interference between access

and backhaul links. All communication links of access and backhaul are separated in different time slots in [6] and in different frequency bands in [7], which will cause low resource utilization. Reference [8] separates access and backhaul in orthogonal mmWave frequency band with the backhaul bandwidth being partitioned among ground small base stations (SBSs) and the access bandwidth being shared. The total bandwidth is dynamically and independently split between access and backhaul by each AP in order to optimize the transmission rate performance [9, 10].

However, the aforementioned works only consider one class of traffic under full-buffer assumption and evaluate rate outage probability and spectrum efficiency without packet level analysis and unsaturated traffic consideration. Currently, user traffic becomes more heterogeneous in the 5G wireless networks such as text data, voice message, video streaming and so on. In addition, different classes of user traffic have different quality-of-service (QoS) requirements. How to allocate communication resources appropriately among heterogeneous traffic to not only enhance the QoS performance of all classes of traffic but also realize performance equilibrium among different classes of user traffic becomes an important issue [11].

In this paper, we develop a theoretical framework to evaluate the mean packet throughput (MPT) of heterogeneous traffic in mmWave UAV-assisted IAB cellular networks. Using stochastic geometry, a system model of the coexistence of UAVs and ground BSs in the network is proposed, where GUEs can establish access transmissions with BSs or UAVs that connect to BSs for backhaul support. By adopting orthogonal spectrum allocation strategy between access and backhaul and equal partition or average load partition spectrum allocation among heterogeneous traffic, this paper provides analytical expressions for MPT based on queueing theory to evaluate the packet transmission performance of different classes of traffic in the downlink communication network. The theoretical derivations are validated by Monte Carlo simulations and the results demonstrate how UAV height, UAV density, and spectrum allocation generate impacts on the MPT performance of heterogeneous traffic in the network of interest.

## II. SYSTEM MODEL

### A. Stochastic Geometry Model and Traffic Model

We consider a mmWave cellular network where ground BSs and UAVs coexist. Ground BSs and UAVs are distributed as homogeneous Poisson point processes (HPPPs)  $\Phi_B$  and  $\Phi_U$

This work was supported in part by the National Natural Science Foundation Program of China (NSFC) under Grants, U21A20456, 61771427, and U21B2029, and in part by a Nokia donation project.

with densities  $\lambda_b$  and  $\lambda_u$ , respectively. Suppose that BSs are all at the same height  $H_B$  and UAVs are all at  $H_U$ . Discrete time system is adopted for the packet transmission analysis in the network and different types of user traffic have different packet arrival probabilities in each time slot. We focus on  $Q$  classes of GUEs which have different types of traffic and thus with different packet arrival rates, which are modeled as Bernoulli processes with probabilities  $\xi_q, q = 1, 2, \dots, Q$ , respectively. The distribution of GUEs of class  $q$  are also modeled as HPPP  $\Phi_{G_q}$  with density  $\lambda_{g_q}, q = 1, 2, \dots, Q$ .

As we focus on downlink transmissions in this paper, our analysis is based on a typical user chosen from  $\Phi_{G_q}$  at random. Let  $u$  denote the typical user itself and its location. We shift our coordinate system origin to the location of the typical user.

### B. Channel Model

For downlink transmissions in the UAV-assisted cellular network, there exist three types of links, including the link from a BS to a GUE (B→G link), the link from a BS to a UAV (B→U link), and the link from a UAV to a GUE (U→G link). Our model takes obstacles in urban environment into consideration and the height of each obstacle follows Rayleigh distribution [12]. Because of the existence of obstacles, whether the link between the typical user and a UAV contains a LoS path follows a certain probability, which is given as [12]

$$P_{\text{LoS}}(r) = \frac{1}{1 + \beta \exp(-\rho(\frac{180}{\pi} \tan^{-1} \frac{H_U}{r} - \beta))} \quad (1)$$

where  $\beta$  and  $\rho$  are obstacle parameters,  $r$  denotes the horizontal distance between the typical user and the UAV.

According to the thinning property of Poisson point process (PPP) and the existence or nonexistence of a LoS path in the link between the typical user and a UAV, all UAVs can be divided into two groups relative to the typical user: the UAVs of a LoS path with the typical user denoted by LoS UAVs as PPP  $\Phi_{U_1}$  with density  $\lambda_{u_1}(r) = P_{\text{LoS}}(r)\lambda_u$  and the UAVs only of NLoS paths denoted by NLoS UAVs as PPP  $\Phi_{U_n}$  with density  $\lambda_{u_n}(r) = (1 - P_{\text{LoS}}(r))\lambda_u$ . Thus, we model the UAV-assisted cellular network as a heterogeneous network of three tiers of APs with respect to the typical user. The positions of each tier's APs are modeled as PPP  $\Phi_j$  with density of  $\lambda_j(r)$ , where  $\lambda_j(r)$  is equal to  $\lambda_b$ ,  $\lambda_{u_1}(r)$ , and  $\lambda_{u_n}(r)$  if  $j = 1$  for ground BSs,  $j = 2$  for LoS UAVs, and  $j = 3$  for NLoS UAVs, respectively.

Nakagami- $m$  fading model is utilized to model the small-scale fading of mmWave access and backhaul links [4]. Since UAVs and BSs both have certain heights, the B→U transmission link can be seen as containing a LoS path. On the other hand, the B→G link is considered as only NLoS paths due to obstacles and the ground deployment of GUEs. Thus, the small-scale fading gains of the B→G link, the link from a NLoS UAV to a GUE ( $U_n \rightarrow G$  link), the link from a LoS UAV to a GUE ( $U_1 \rightarrow G$  link), and the B→U link are modeled as random variables following gamma distribution, where the former two can be specialized as exponential distribution because of the nonexistence of a LoS path.

MmWave wireless communication uses directional beamforming to overcome the huge propagation loss. Therefore, we assume that BSs and UAVs are all equipped with directional antenna arrays [9]. The main lobe antenna gains of BSs, LoS UAVs, and NLoS UAVs are denoted as  $G_j$  within beamwidth  $\theta_j$ , and the side lobe antenna gains are  $g_j, j = 1, 2, 3$ , respectively, given  $G_1 = G_B, G_2 = G_3 = G_U, \theta_1 = \theta_B, \theta_2 = \theta_3 = \theta_U, g_1 = g_B$ , and  $g_2 = g_3 = g_U$ . Similar to [8, 9], we consider that GUEs are equipped with omnidirectional antennas with antenna gain  $G_G$ . The illustration of antenna gains is shown in Fig. 1.

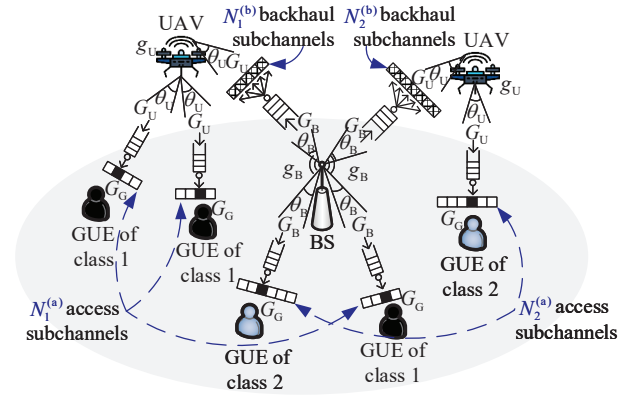


Fig. 1. Illustration of antenna gains and traffic of the network for  $Q = 2$ .

### C. Spectrum Allocation

The total spectrum resource is orthogonally partitioned by access and backhaul links with coefficient  $\eta$  based on IAB. The total bandwidth  $B$  is separated into  $N$  subchannels and each subchannel has a bandwidth of  $B_0 = B/N$ . Consider that the B→G and U→G access links share the  $N^{(a)} = \eta N$  access subchannels. Similarly, all UAVs share the same  $N^{(b)} = (1 - \eta)N$  backhaul subchannels to communicate with BSs. The total  $N^{(a)}$  access and  $N^{(b)}$  backhaul subchannels are allocated to each class of users based on equal partition or average load partition strategies.  $N_q^{(a)} = \frac{N^{(a)}}{Q}$  or  $N_q^{(a)} = \frac{\xi_q}{\sum_{q=1}^Q \xi_q} N^{(a)}$  access subchannels and  $N_q^{(b)} = \frac{N^{(b)}}{Q}$  or  $N_q^{(b)} = \frac{\xi_q}{\sum_{q=1}^Q \xi_q} N^{(b)}$  backhaul subchannels are allocated to the  $q^{\text{th}}$  class users according to average split or the average load of APs caused by the  $q^{\text{th}}$  class users, i.e., the packet arrival rate  $\xi_q$ , respectively. In each time slot, a BS or UAV assigns the  $N_q^{(a)}$  access subchannels randomly to its associated  $q^{\text{th}}$  class GUEs with non-empty packet queues. Assume that a GUE with an allocated subchannel can receive one data packet in a time slot if the involved transmission is successful.

### D. User Association

The typical user associates with a UAV or BS based on the maximum average received power association strategy. The associated UAV or BS of the typical user is denoted as the tagged UAV or BS. We denote the location of the tagged AP as  $\mathbf{x}^*$ , which is in the  $k^{\text{th}}$  tier, as for  $k=1$  being the BS tier,  $k=2$  being LoS UAVs, and  $k=3$  being NLoS UAVs. For simplicity,

$\mathbf{x}^*$  is also used as the tag of the tagged UAV or BS. The received power at the typical user from  $\mathbf{x}^*$  is given by

$$P_{r,k}(X_k) = P_{t,k} h_{k,\mathbf{u}} \psi_{k,G} \zeta X_k^{-\alpha_k} \quad (2)$$

where  $P_{t,k}$  is the transmit power of the  $k^{\text{th}}$  tier APs,  $X_k = \|\mathbf{x}^*\|$  is the distance between the tagged AP and the typical user,  $h_{k,\mathbf{u}}$  is the small-scale fading gain from the tagged AP in the  $k^{\text{th}}$  tier to the typical user on the subchannel allocated to  $\mathbf{u}$ ,  $\psi_{k,G} = G_k G_G$  denotes the antenna gain of the transmission links between the  $k^{\text{th}}$  tier APs and the typical user,  $\zeta = (\frac{3 \times 10^8}{4\pi f_c})^2$  is the path loss intercept with  $f_c$  being the carrier frequency, and  $\alpha_k$  denotes the path loss exponent of the links from the  $k^{\text{th}}$  tier APs to the typical user. Considering the average received power, we have  $\bar{P}_{r,k}(X_k) = T_k X_k^{-\alpha_k}$ , where  $T_k = P_{t,k} \bar{h}_{k,\mathbf{u}} \psi_{k,G} \zeta$  with  $\bar{h}_{k,\mathbf{u}}$  denoting the average small-scale fading gain from the tagged AP to the typical user.

Let  $L_j$  denote the minimum distance between the typical user and the  $j^{\text{th}}$  tier APs. The association probability of the typical user associated with the tagged UAV or BS  $\mathbf{x}^*$  in the  $k^{\text{th}}$  tier can be derived as

$$A_k = \mathbb{E}_{L_k}[\bar{P}_{r,k}(L_k) > \max_{j \in \{1,2,3\}, j \neq k} \bar{P}_{r,j}(L_j)] \quad (3)$$

$$= 2\pi \int_0^\infty \lambda_k(r) r \exp \left\{ -2\pi \sum_{j=1}^3 \int_0^{\hat{r}_j} \lambda_j(r) r dr \right\} dr$$

where  $r$  is the horizontal distance between the tagged AP and the typical user,  $\hat{r}_j = \sqrt{(\frac{T_j}{T_k})^{\frac{2}{\alpha_j}} (r^2 + H_k^2)^{\frac{\alpha_k}{\alpha_j}} - H_j^2}$  denotes the minimum horizontal distance between the  $j^{\text{th}}$  tier APs and the typical user with  $H_k = H_j = \begin{cases} H_B, & \text{if } k, j = 1 \\ H_U, & \text{if } k, j = 2, 3 \end{cases}$ .

The probability density function (PDF) of the distance  $X_k$  between the typical user and the tagged UAV or BS in the  $k^{\text{th}}$  tier is given by [4]

$$f_{X_k}(x) = \frac{2\pi}{A_k} \lambda_k(\sqrt{x^2 - H_k^2}) x \exp \left\{ -2\pi \sum_{j=1}^3 \int_0^{\hat{x}_j} \lambda_j(r) r dr \right\} \quad (4)$$

where  $\hat{x}_j = \sqrt{(\frac{T_j}{T_k})^{\frac{2}{\alpha_j}} x^{\frac{2\alpha_k}{\alpha_j}} - H_j^2}$ .

We consider that UAVs are served by their nearest BSs. Let  $\Delta H = H_U - H_B$  denote the height difference between UAVs and BSs. The PDF of the distance  $Z$  between the tagged UAV and its nearest BS can be derived according to (4) as [4]

$$f_Z(z) = 2\pi \lambda_b z \exp(-\pi \lambda_b (z^2 - \Delta H^2)). \quad (5)$$

Assume that the total number of GUEs of class  $q$  associated with the  $k^{\text{th}}$  tier tagged AP is  $M_{k,q,0}$ . Its probability mass function (PMF) is given as [13]

$$\mathbb{P}(M_{k,q,0} = m) = \begin{cases} \frac{3.5^{3.5} \Gamma(m+3.5) (\frac{\lambda_{gq} A_1}{\lambda_b})^m}{m! \Gamma(3.5) (3.5 + \frac{\lambda_{gq} A_1}{\lambda_b})^{m+3.5}}, & k = 1 \\ \frac{3.5^{3.5} \Gamma(m+3.5) \left[ \frac{\lambda_{gq} (A_2 + A_3)}{\lambda_u} \right]^m}{m! \Gamma(3.5) \left[ 3.5 + \frac{\lambda_{gq} (A_2 + A_3)}{\lambda_u} \right]^{m+3.5}}, & k = 2, 3 \end{cases}, m \geq 0 \quad (6)$$

where  $\Gamma(\cdot)$  is the gamma function. The maximum numbers of each class of users associated with BSs, LoS UAVs and NLoS UAVs are defined as  $M_{1,\max} = M_{B,\max}$  and  $M_{2,\max} = M_{3,\max} = M_{U,\max}$ , respectively, due to the limited capacity of BSs and UAVs.  $M_{B,\max}$  or  $M_{U,\max}$  users are selected at random if the total number of the some class of users associated with a BS or UAV exceeds the maximum value. Thus, the PMF of  $M_{k,q}$  which is the number of successfully associated users of class  $q$  of the tagged AP is given by

$$\mathbb{P}(M_{k,q} = m) = \begin{cases} \mathbb{P}(M_{k,q,0} = m), & m = 0, 1, \dots, M_{k,\max} - 1 \\ \sum_{m'=m}^\infty \mathbb{P}(M_{k,q,0} = m'), & m = M_{k,\max}. \end{cases} \quad (7)$$

### III. MEAN PACKET THROUGHPUT ANALYSIS

In this section, we develop a theoretical framework to study the mean packet throughput of heterogeneous traffic for mmWave UAV-assisted IAB cellular networks by leveraging stochastic geometry and queueing theory.

#### A. Signal to Interference plus Noise Ratio

GUEs can receive signals not only from their associated BSs or UAVs, but also from other nearby APs. Because of the spectrum sharing between B→G and U→G access links, the interference among access links on the same subchannel should be considered. The signal to interference plus noise ratio (SINR) at the typical user  $\mathbf{u}$  served by the tagged UAV or BS in the  $k^{\text{th}}$  tier can be expressed as

$$\gamma_{k,\mathbf{u}}^{(a)} = \frac{P_{t,k} h_{k,\mathbf{u}} \psi_{k,G} \zeta X_k^{-\alpha_k}}{\sum_{j=1}^3 \sum_{\mathbf{x}_i \in \Phi_j \setminus \mathbf{x}^*} \delta_{j,i,\mathbf{u}} P_{t,j} h_{j,i,\mathbf{u}} \psi_{j,G}^{(1)} \zeta Y_{j,i}^{-\alpha_j} + \sigma_0 B_0} \quad (8)$$

where  $\delta_{j,i,\mathbf{u}}$  denotes whether the  $i^{\text{th}}$  AP in the  $j^{\text{th}}$  tier is sending packets on the same subchannel allocated to the typical user  $\mathbf{u}$  by the tagged AP,  $h_{j,i,\mathbf{u}}$  is the small-scale fading gain on the subchannel allocated to the typical user  $\mathbf{u}$  from the  $i^{\text{th}}$  AP in the  $j^{\text{th}}$  tier to the typical user,  $\psi_{j,G}^{(1)}$  denotes the interfering antenna gain from the  $i^{\text{th}}$  AP in the  $j^{\text{th}}$  tier to the typical user, which is a discrete random variable equal to  $G_j G_G$  or  $g_j G_G$  with probability  $p_{j,G}^{(1)}$  equal to  $\frac{\theta_j}{2\pi}$  or  $1 - \frac{\theta_j}{2\pi}$ ,  $Y_{j,i}$  is the distance between the  $i^{\text{th}}$  AP in the  $j^{\text{th}}$  tier and the typical user, and  $\sigma_0$  is the noise power spectral density.

Due to the high beamforming capability of BSs and UAVs, similar to [9], we assume backhaul links are noise-limited, meaning that the interference among B→U links can be ignored. Then, the signal to noise ratio (SNR) received by the tagged UAV from its nearest BS can be expressed as

$$\gamma^{(b)} = \frac{P_{t,1} h_{B,U} \psi_{B,U} \zeta Z^{-\alpha_4}}{\sigma_0 B_0} \quad (9)$$

where  $h_{B,U}$ ,  $\psi_{B,U} = G_B G_U$ , and  $\alpha_4$  denote the small-scale fading gain, the antenna gain, and the path loss exponent of the backhaul link between the tagged UAV and its nearest BS, respectively.

### B. Packet Queueing Model of Access Links

In this and the next subsection, we illustrate the packet transmission of the UAV-assisted IAB cellular network and analyze packet queueing models. An example where users are of two classes of traffic is shown in Fig. 1.

Discrete time queueing model is adopted to model the packet arrivals and departures of the access links of the tagged AP and the interfering APs [14]. We divide the continuous time into discrete time slots and a packet arrives or leaves with a certain probability in each time slot. Specifically, for the  $n^{\text{th}}$  time slot, packet arrivals and departures take place in the interval  $(n, n^+)$  and  $(n^-, n)$ , respectively. The number of packets in the queueing system at moment  $n^+$  denotes the state of the queueing system in the  $n^{\text{th}}$  time slot.

The packet queueing system from the tagged AP or an interfering AP to the typical user is modeled as a Geom/Geom/1 queue. Packets of the  $q^{\text{th}}$  class users arrive at a queue in each time slot with the probability of  $\xi_q$  and packets leave a queue according to first-in first-out (FIFO) scheduling. If a packet fails to leave in a time slot, it would stay at the head of the queue and be retransmitted in next available time slot. We take the typical user from class  $q$  as an example to analyze the packet queueing system.

Whether the tagged BS or UAV can successfully transmit a packet to the typical user depends on the subchannel contention and communication environment. A GUE who has packet(s) to receive from its serving AP (or denoted as an active user) would contend for a subchannel. The probability  $p_{k,q,M_{k,q}}$  that the tagged AP in the  $k^{\text{th}}$  tier with  $M_{k,q}$  successfully associated  $q^{\text{th}}$  class users may allocate a subchannel to the typical user for packet transmission is given by

$$p_{k,q,M_{k,q}} = \min \left\{ \frac{N_q^{(a)}}{(1 - Q_{k,q,M_{k,q}}(0))(M_{k,q} - 1) + 1}, 1 \right\} \quad (10)$$

where, according to the property of Geom/Geom/1 queue,  $Q_{k,q,M_{k,q}}(0) = 1 - \frac{\xi_q}{\mu_{k,q,M_{k,q}}^{(a)}}$  is the probability that the Geom/Geom/1 queueing system of the typical user is empty, with  $\mu_{k,q,M_{k,q}}^{(a)}$  being the packet service rate of the Geom/Geom/1 queueing system from the tagged AP to the typical user. Thus,  $(1 - Q_{k,q,M_{k,q}}(0))(M_{k,q} - 1)$  is the average number of the active users of class  $q$  served by the tagged BS or UAV except the active typical user.

The packet service rate  $\mu_{k,q,M_{k,q}}^{(a)}$  is equivalent to the probability that the tagged BS or UAV allocates a subchannel to the typical user and the transmission of a packet on the allocated subchannel is successful, which can be derived as

$$\mu_{k,q,M_{k,q}}^{(a)} = p_{k,q,M_{k,q}} \mathbb{P}(\gamma_{k,u}^{(a)} > \tau_a) \quad (11)$$

where  $\mathbb{P}(\gamma_{k,u}^{(a)} > \tau_a)$  is the probability that a packet can be successfully transmitted from the tagged AP to the typical user on the subchannel allocated to the typical user  $u$ , and  $\tau_a$  is the SINR threshold that GUEs can successfully receive packets from APs. As  $h_{k,u}$  in (8) is gamma distributed,  $\mathbb{P}(\gamma_{k,u}^{(a)} > \tau_a)$  can be further derived based on stochastic geometry as [15]

$$\mathbb{P}(\gamma_{k,u}^{(a)} > \tau_a) = \int_{H_k} \sum_{n=0}^{m_k-1} \frac{s_k^n}{n!} \exp(-s_k \sigma_0 B_0) \sum_{d=0}^n (-1)^{2n-d} \cdot C_n^d \sigma_0^{n-d} B_0^{n-d} \frac{d^d \mathcal{L}_I(s_k)}{ds_k^d} f_{X_k}(x) dx \quad (12)$$

where  $s_k = \frac{m_k \tau_a}{P_{t,k} \psi_{k,G} \zeta X_k^{-\alpha_k}}$ ,  $m_k$  is the Nakagami- $m$  fading parameter of the link between the tagged AP in the  $k^{\text{th}}$  tier and the typical user, and  $f_{X_k}(x)$  is shown in (4). Due to space limitation, we omit the proof of (12). The interested reader can refer to [15] for a similar proof. In (12),  $\mathcal{L}_I(s_k)$  derived from the probability generating functional of PPP is given by (13) as shown at the bottom of this page, where  $y_{\min} = \left(\frac{T_j}{T_k}\right)^{\frac{1}{\alpha_j}} X_k^{\frac{\alpha_k}{\alpha_j}}$ ,  ${}_2F_1(\cdot)$  is the Gaussian hypergeometric function, and  $\mathbb{P}_q(\delta_{j,i,u} = 1)$  represents the probability that the  $i^{\text{th}}$  AP in the  $j^{\text{th}}$  tier has packet(s) to send on the same subchannel allocated to the typical user and is given by

$$\mathbb{P}_q(\delta_{j,i,u} = 1) = \sum_{m'=1}^{M_{j,\max}} \min \left\{ \frac{m' \xi_q}{\mu_{j,q,m'}^{(a)} N_q^{(a)}}, 1 \right\} \cdot \mathbb{P}(M_{j,q} = m') \quad (14)$$

with  $M_{j,q}$  being the number of the  $q^{\text{th}}$  class users successfully associated with the  $i^{\text{th}}$  interfering AP in the  $j^{\text{th}}$  tier,  $\mu_{j,q,m'}^{(a)}$  being the packet service rate of the queueing system from the interfering AP to one of its active associated users, depending on whether the interfering AP is able to allocate a subchannel to the user and the packet can be successfully transmitted. Due to the same analysis and derivation process, we can obtain  $\mu_{j,q,M_{j,q}}^{(a)}$  similar to  $\mu_{k,q,M_{k,q}}^{(a)}$  in (11).

According to Little's law, the average time  $W_{k,q,M_{k,q}}^{(a)}$  that a packet of the typical user spends in the queueing system of the access link equals the average number of packets  $L_{k,q,M_{k,q}}^{(a)}$  in the access queueing system divided by the packet arrival rate. With some derivations, we have

$$W_{k,q,M_{k,q}}^{(a)} = \frac{L_{k,q,M_{k,q}}^{(a)}}{\xi_q} = \frac{1 - \xi_q}{\mu_{k,q,M_{k,q}}^{(a)} - \xi_q}. \quad (15)$$

$$\mathcal{L}_I(s_k) = \prod_{j=1}^3 \exp \left[ \frac{2\pi \mathbb{P}_q(\delta_{j,i,u}=1) \int_0^\infty \lambda_j(r) r dr}{\alpha_j \int_0^\infty r dr} \left( \frac{\frac{\theta_j}{2\pi} \sum_{t=1}^{m_j} C_{m_j}^t (-1)^t \frac{y_{\min}^{2-\alpha_j t} (P_{t,j} G_j G_G \zeta s_k)^t}{(t - \frac{2}{\alpha_j}) m_j^t} {}_2F_1(t, t - \frac{2}{\alpha_j}; t - \frac{2}{\alpha_j} + 1; -\frac{P_{t,j} G_j G_G \zeta s_k}{m_j y_{\min}^{\alpha_j}}) + (1 - \frac{\theta_j}{2\pi}) \sum_{t=1}^{m_j} C_{m_j}^t (-1)^t \frac{y_{\min}^{2-\alpha_j t} (P_{t,j} g_j G_G \zeta s_k)^t}{(t - \frac{2}{\alpha_j}) m_j^t} {}_2F_1(t, t - \frac{2}{\alpha_j}; t - \frac{2}{\alpha_j} + 1; -\frac{P_{t,j} g_j G_G \zeta s_k}{m_j y_{\min}^{\alpha_j}}) \right) \right]. \quad (13)$$

### C. Packet Queueing Model of Backhaul Links

Due to the co-channel spectrum sharing among backhaul links, each link between BSs and UAVs occupies the same  $N^{(b)}$  backhaul subchannels, which is noise-limited. Thus, the packet service rate  $\mu^{(b)}$  on a subchannel of the backhaul link from the nearest BS to the tagged UAV is equal to the probability that the nearest BS can successfully transmit a packet to the tagged UAV, which can be derived by using stochastic geometry-based analysis as

$$\begin{aligned} \mu^{(b)} &= \mathbb{P}(\gamma^{(b)} > \tau_b) \\ &= \int_{\Delta H}^{\infty} 2\pi\lambda_b z \sum_{n=0}^{m_4-1} \frac{(m_4 \frac{\tau_b \sigma_0 B_0}{P_{t,1} \psi_{B,U} \zeta z^{-\alpha_4}})^n}{n!} \\ &\quad \exp(-m_4 \frac{\tau_b \sigma_0 B_0}{P_{t,1} \psi_{B,U} \zeta z^{-\alpha_4}} - \pi\lambda_b z^2) dz \end{aligned} \quad (16)$$

where  $m_4$  is the Nakagami- $m$  fading parameter of the backhaul link between the tagged UAV and its nearest BS, and  $\tau_b$  is the SNR threshold that UAVs can successfully receive packets from BSs.

The packet queueing process of the backhaul link between the tagged UAV and its nearest BS is modeled as  $Q$  large queues for packets of  $Q$  classes of users. Based on FIFO scheduling, all packets arriving at the BS of the  $q^{\text{th}}$  class users successfully associated with the tagged UAV are stored in the  $q^{\text{th}}$  large queue. Generally, the probability that two or more packets arrive simultaneously at a queue is small. Thus, we assume that at most one packet arrives per time slot and the total packet arrival rate of the  $q^{\text{th}}$  large queue is  $\xi_q M_{k,q}$  conditioned on  $M_{k,q}$  successfully associated users of class  $q$  of the tagged UAV.

Then, the packet queue for the  $q^{\text{th}}$  class users from the nearest BS to the tagged UAV is characterized as a Geom/Geom/ $s$  queue with packet arrival rate  $\xi_q M_{k,q}$  and  $s = N_q^{(b)}$  servers. Here,  $N_q^{(b)}$  is the number of backhaul subchannels allocated to the  $q^{\text{th}}$  class GUEs, namely the number of queue servers of class  $q$  users, with each server having a packet service rate  $\mu^{(b)}$ . The stationary probabilities  $\pi_{q,d}$  that there are  $d$  packets in the queueing system of class  $q$  users can be calculated according to the property of Geom/Geom/ $s$  queue provided that the queue is stable [16], i.e.,  $\xi_q M_{k,q} < N_q^{(b)} \mu^{(b)}$ .

According to Little's law, the average time  $W_{k,q,M_{k,q}}^{(b)}$  that a packet of class  $q$  users spends in the queueing system of the backhaul link is the average number of packets  $L_{k,q,M_{k,q}}^{(b)}$  in the backhaul queueing system divided by total packet arrival rate, i.e.,

$$W_{k,q,M_{k,q}}^{(b)} = \frac{L_{k,q,M_{k,q}}^{(b)}}{\xi_q M_{k,q}} = \frac{\sum_{d=0}^{\infty} \pi_{q,d} d}{\xi_q M_{k,q}}. \quad (17)$$

### D. Mean Packet Throughput

MPT denoted by  $T$  is the reciprocal of the average time that a packet spends in the queueing system. Conditioned on  $M_{k,q}$ , the MPT of the typical user of class  $q$  associated with the tagged AP in the  $k^{\text{th}}$  tier  $T_{k,q,M_{k,q}}$  is given by

$$T_{k,q,M_{k,q}} = \begin{cases} \frac{1}{W_{k,q,M_{k,q}}^{(a)}}, & \text{if } \mu_{k,q,M_{k,q}}^{(a)} > \xi_q, k=1 \\ \frac{1}{W_{k,q,M_{k,q}}^{(a)} + W_{k,q,M_{k,q}}^{(b)}}, & \text{if } N_q^{(b)} \mu^{(b)} > \xi_q M_{k,q} \text{ and } \mu_{k,q,M_{k,q}}^{(a)} > \xi_q, k=2,3 \\ 0, & \text{if } N_q^{(b)} \mu^{(b)} \leq \xi_q M_{k,q} \text{ or } \mu_{k,q,M_{k,q}}^{(a)} \leq \xi_q, k=1,2,3. \end{cases} \quad (18)$$

Then, by averaging on the tagged AP's tier choice and the number of its successfully associated users, the MPT of the typical user of class  $q$  can be given by

$$T_q = \sum_{k=1}^3 A_k \sum_{m=1}^{M_{k,\max}} \frac{\mathbb{P}(M_{k,q} = m)}{1 - \mathbb{P}(M_{k,q} = 0)} T_{k,q,m} \quad (19)$$

where  $T_{k,q,M_{k,q}}$  equals  $T_{k,q,m}$  when  $M_{k,q} = m$ .

## IV. NUMERICAL RESULTS AND DISCUSSIONS

In this section, we provide numerical results to investigate the MPT performance of heterogeneous traffic of the UAV-assisted IAB cellular network. The theoretical analysis is validated through 1000 Monte Carlo simulation realizations. The simulation area is  $1000 \times 1000$  m<sup>2</sup> and each realization includes 5000 continuous time slots. Unless otherwise stated, the simulation parameters are as follows [4]:  $\lambda_b = 2 \times 10^{-5}$ /m<sup>2</sup>,  $\lambda_u = 1 \times 10^{-4}$ /m<sup>2</sup>,  $\lambda_{g,q} = 3 \times 10^{-3}$ /m<sup>2</sup>,  $H_B = 10$  m,  $\beta = 11.95$ ,  $\rho = 0.136$ ,  $P_{t,1} = 40$  dBm,  $P_{t,2} = P_{t,3} = 30$  dBm,  $G_B = G_U = 18$  dB,  $G_G = 0$  dB,  $\theta_B = \theta_U = 20^\circ$ ,  $g_B = g_U = -2$  dB,  $\alpha_1 = \alpha_3 = 4$ ,  $\alpha_2 = \alpha_4 = 3$ ,  $m_1 = m_3 = 1$ ,  $m_2 = m_4 = 3$ ,  $M_{B,\max} = 100$ ,  $M_{U,\max} = 10$ ,  $f_c = 28$  GHz,  $B = 3$  GHz,  $N = 15$ ,  $\sigma_0 = -174$  dBm/Hz,  $\tau_a = 0$  dB,  $\tau_b = 10$  dB,  $Q = 3$ ,  $\xi_1 = 0.1$ ,  $\xi_2 = 0.07$ , and  $\xi_3 = 0.03$ .

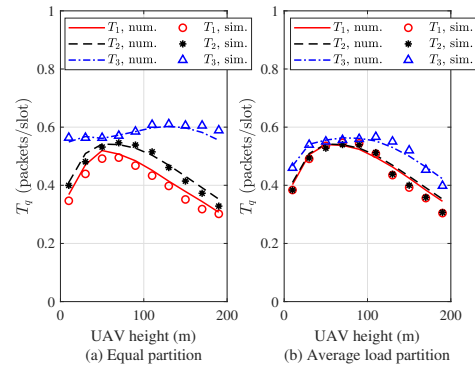


Fig. 2. MPT vs. UAV height under different spectrum allocation strategies among heterogeneous traffic.

In Fig. 2, we validate the numerical results obtained from the above theoretical analysis by simulation results and study the impacts of UAV height and spectrum allocation strategy among heterogeneous traffic on MPT performance of users, given the allocation coefficient between access and backhaul  $\eta$  equal to 0.6. In the figure, one can notice that the MPT of users, except for the 3<sup>rd</sup> class users and under the equal partition strategy, increases first and then decreases with an increase of UAV height. This is because, when UAVs are at



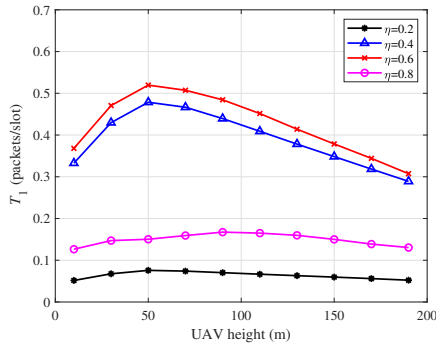


Fig. 3. MPT of the 1<sup>st</sup> class users vs. UAV height under different spectrum allocation coefficients between access and backhaul.

a low altitude, they can not only establish LoS paths with GUEs but also cause serious interference with each other. On the other hand, when they are at a high altitude, the path loss dominates and the transmission quality of access and backhaul links degrades, thus degrading the MPT performance. Due to the lowest packet arrival rate and abundant subchannels, the MPT performance of the 3<sup>rd</sup> class users has strong tolerance of interference and path loss under equal partition. However, with the average load partition strategy which reduces the 3<sup>rd</sup> class users' subchannels, Fig. 2(b) shows more equitable MPT performance among heterogeneous traffic by achieving a balance between resource demand and subchannel allocation.

In Fig. 3, we take the 1<sup>st</sup> class users as an example to study the impact of different spectrum allocation coefficients between access and backhaul on MPT based on average load partition among heterogeneous traffic. Fig. 3 illustrates that few subchannels for access or backhaul will lead to bad MPT performance because of the transmission bottleneck caused by access or backhaul links. Proper allocation coefficient between access and backhaul can improve network performance, which is also verified in [8]. Due to the directional transmission of backhaul links, allocating fewer spectrum resources to backhaul and more to access enables better QoS guarantee.

In Fig. 4, we study the impact of different density ratios of BSs to UAVs on MPT under the condition of average load partition among heterogeneous traffic and coefficient  $\eta$  equal to 0.6. As shown in Fig. 4, with the increase of the density ratio of BSs to UAVs, the MPT improves before reaching a critical value. However, continuing to increase the ratio does not improve the MPT performance. Instead, the MPT would degrade due to the increase of interference caused by massive UAVs. We also study the ground SBS-assisted network instead of UAVs. As seen from Fig. 4, the deployment of SBSs on the ground does not improve the MPT performance as good as UAVs unless with an extremely high density. This is because that the transmissions of ground SBSs suffer greatly from obstacles while proper UAV positions can establish LoS paths with GUEs more easily.

## V. CONCLUSION

In this paper, we have proposed an analytical framework to study the QoS performance of heterogeneous traffic for mmWave UAV-assisted IAB cellular networks. Using stochastic geometry and queueing theory, we have analyzed the mean

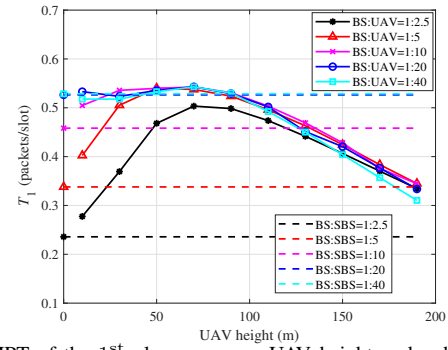


Fig. 4. MPT of the 1<sup>st</sup> class users vs. UAV height under different density ratios of BSs to UAVs.

packet throughput of different classes of users under equal and average load spectrum partition and validated our results by Monte Carlo simulations. The numerical results show that UAV height, UAV density, and spectrum allocation between access and backhaul and among heterogeneous traffic have significant influences on the MPT performance of the network.

## REFERENCES

- [1] Mozaffari *et al.*, "A tutorial on UAVs for wireless networks: Applications, challenges, and open problems," *IEEE Commun. Surv. Tutor.*, vol. 21, no. 3, pp. 2334–2360, 3rd Quart., 2019.
- [2] Z. Xiao, P. Xia, and X.-G. Xia, "Enabling UAV cellular with millimeter-wave communication: Potentials and approaches," *IEEE Commun. Mag.*, vol. 54, no. 5, pp. 66–73, May 2016.
- [3] G. Zhang, *et al.*, "Fundamentals of heterogeneous backhaul design—analysis and optimization," *IEEE Trans. Commun.*, vol. 64, no. 2, pp. 876–889, Feb. 2016.
- [4] N. Kouzayha *et al.*, "Analysis of large scale aerial terrestrial networks with mmWave backhauling," *IEEE Trans. Wireless Commun.*, pp. 1–1, Jul. 2021.
- [5] C. Dehos *et al.*, "Millimeter-wave access and backhauling: the solution to the exponential data traffic increase in 5G mobile communications systems?" *IEEE Commun. Mag.*, vol. 52, no. 9, pp. 88–95, Sep. 2014.
- [6] Y. Liu *et al.*, "Joint incentive and resource allocation design for user provided network under 5G integrated access and backhaul networks," *IEEE Trans. Netw. Sci. Eng.*, vol. 7, no. 2, pp. 673–685, Apr. 2019.
- [7] J. Y. Lai, W.-H. Wu, and Y. T. Su, "Resource allocation and node placement in multi-hop heterogeneous integrated-access-and-backhaul networks," *IEEE Access*, vol. 8, pp. 122 937–122 958, Jul. 2020.
- [8] C. Saha *et al.*, "Bandwidth partitioning and downlink analysis in millimeter wave integrated access and backhaul for 5G," *IEEE Trans. Wireless Commun.*, vol. 17, no. 12, pp. 8195–8210, Dec. 2018.
- [9] C. Saha and H. S. Dhillon, "Millimeter wave integrated access and backhaul in 5G: Performance analysis and design insights," *IEEE J. Sel. Areas Commun.*, vol. 37, no. 12, pp. 2669–2684, Dec. 2019.
- [10] W. Lei, Y. Ye, and M. Xiao, "Deep reinforcement learning-based spectrum allocation in integrated access and backhaul networks," *IEEE Trans. Cogn. Commun. Netw.*, vol. 6, no. 3, pp. 970–979, Sep. 2020.
- [11] X. Ma *et al.*, "Resource allocation for heterogeneous applications with device-to-device communication underlying cellular networks," *IEEE J. Sel. Areas Commun.*, vol. 34, no. 1, pp. 15–26, Jan. 2016.
- [12] Al-Hourani *et al.*, "Optimal LAP altitude for maximum coverage," *IEEE Wirel. Commun. Lett.*, vol. 3, no. 6, pp. 569–572, Dec. 2014.
- [13] J. Li *et al.*, "Analysis of packet throughput in small cell networks under clustered dynamic TDD," *IEEE Trans. Wireless Commun.*, vol. 17, no. 9, pp. 5729–5742, Sep. 2018.
- [14] M. Song *et al.*, "Throughput analysis of small cell networks under D-TDD and FFR," *IEEE Communications Letters*, vol. 25, no. 2, pp. 665–669, Feb. 2021.
- [15] B. Galkin, J. Kibilda, and L. A. DaSilva, "A stochastic model for UAV networks positioned above demand hotspots in urban environments," *IEEE Trans. Veh. Technol.*, vol. 68, no. 7, pp. 6985–6996, Jul. 2019.
- [16] A. S. Alfa, *Applied Discrete-Time Queues*, New York, NY, USA: Springer, 2016.